# NONLINEAR-PHASE BASIS FUNCTIONS IN QUASI-BANDLIMITED OSCILLATOR ALGORITHMS

*Jussi Pekonen*
Independent
http://www.pekonen.cc/
Espoo, Finland
jussi@pekonen.cc

*Martin Holters*
Department of Signal Processing and Communications,
Helmut Schmidt University,
Hamburg, Germany
martin.holters@hsu-hh.de

## ABSTRACT

Virtual analog synthesis requires bandlimited source signal algorithms. An efficient methodology for the task expresses the traditionally used source waveforms or their time-derivatives as a sequence of bandlimited impulses or step functions. Approximations of the ideal bandlimited functions used in these quasi-bandlimited oscillator algorithms are typically linear-phase functions. In this paper, a general nonlinear-phase approach to the task is proposed. The discussed technique transforms an analog prototype filter to a digital filter using a modified impulse invariance transformation method that enables the impulse response to be sampled with arbitrary sub-sample shifts. The resulting digital filter is a set of parallel first- and/or second-order filters that are excited with short burst-like signals that depend on the offset of the waveform discontinuities. The discussed approach is exemplified with a number of design cases, illustrating different trade-offs between good alias reduction and low computational cost.

## 1. INTRODUCTION

Virtual analog synthesizers have become an important part of music synthesizer business. These software synthesizers emulate the subtractive sound synthesis principle utilized in early analog synthesizers of the 1960s and 1970s using digital signal processing methods. In subtractive sound synthesis, a spectrally rich source signal is filtered with a time-varying lowpass filter that has a controllable resonance. Traditionally, the source signal is a periodic classical waveform, such as the sawtooth, rectangular, or triangle wave, or a mix of the aforementioned waveforms [1, 2].

In virtual analog synthesis, it is necessary to have bandlimited oscillator algorithms for the source signals. Trivial digital generation of the periodic classical waveforms suffers from aliasing distortion that is caused by the discontinuities in the waveform or waveform derivative, which effectively produce an infinite number of harmonic components [3–6]. Furthermore, since the spectra of the classical waveforms decay gently, the aliasing distortion becomes clearly audible especially at high fundamental frequencies. Figure 1 shows an example of the aliasing problem with a rectangular waveform having fundamental frequency $f_0 = 3.0$ kHz and a duty cycle (or pulse width) of 25%. Sampling rate $f_s = 44.1$ kHz is used in the example. The crosses in Fig. 1(b) indicate the non-aliased components, the rest of the spectrum is aliasing distortion.

Many discrete-time methods that generate classical-waveform-like signals containing less aliasing than the trivially sampled waveforms have been developed. These methods approach the aliasing problem from different viewpoints and the level of aliasing is reduced differently in each method. The applied techniques can be roughly categorized into four different groups [7–12]:

1. ideally bandlimited algorithms,
2. quasi-bandlimited algorithms,
3. alias-suppressing algorithms, and
4. ad-hoc algorithms.

The ideally bandlimited methods generate only a predefined, fixed number of harmonic components, resulting in completely alias-free waveforms. The quasi-bandlimited algorithms synthesize signals that contain aliasing mainly at high frequencies where human hearing is less sensitive to aliasing distortion than at low and middle frequencies. The alias-suppressing methods have aliasing in the whole audio band but suppressed compared to the trivial approach. The ad-hoc algorithms produce classical-waveform-like signals using simple (nonlinear) processing techniques.

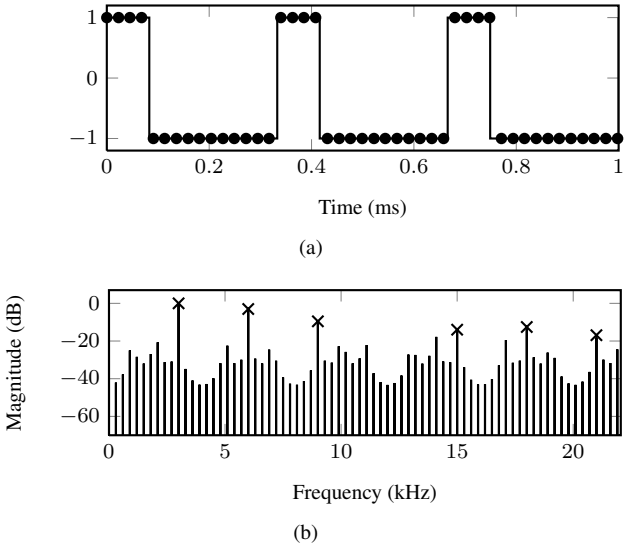


Figure 1: (a) Waveform of a continuous-time rectangular waveform (solid line) having fundamental frequency $f_0 = 3.0$ kHz and a duty cycle of 25% and (b) the spectrum of its trivially sampled digital representation. The dots in (a) represent the sampled data when the sampling rate $f_s$ is 44.1 kHz. The crosses in (b) indicate the non-aliased harmonics components of the digital signal. Note that due to the choice of duty cycle no harmonic is present at 12 kHz.

The first three algorithm groups can be interpreted to have a close connection to the sampling of continuous-time signals. The alias-suppressing methods can be understood to sample a signal that has the same spectral content as the target waveform but whose spectrum rolls off at a steeper rate than the target, hence resulting in a lowered aliasing distortion [7, 9, 11, 12]. The ideally bandlimited algorithms, in turn, simulate the sampling of ideally lowpass-filtered classical waveforms [7, 11, 12].

The quasi-bandlimited methods can also be interpreted to sample lowpass-filtered continuous-time waveforms. However, the lowpass filter is not the ideal filter, like in the ideally bandlimited algorithms, but a realizable filter that has a non-infinitesimal transition band [7, 8, 11–13]. The discrete-time quasi-bandlimited oscillator algorithms proposed so far typically use linear-phase approximations of the impulse or unit step response of the ideal lowpass filter. In this paper, nonlinear-phase approximations of the ideal filter responses, the basis functions of quasi-bandlimited algorithms, are discussed and their applicability to the alias reduction task is investigated.

The remainder of this paper is organized as follows. Section 2 provides the mathematical motivation of the quasi-bandlimited oscillator algorithms by reviewing the derivation of the ideal basis functions. The previously proposed approximations of the ideal basis functions are also briefly discussed. In Sec. 3, the use of nonlinear-phase basis functions in quasi-bandlimited oscillator algorithms is discussed. A time-varying extension to the proposed approach is presented in Sec. 4. In addition, design examples are provided. Finally, Sec. 5 concludes the paper.

## 2. QUASI-BANDLIMITED OSCILLATOR ALGORITHMS

The concept of quasi-bandlimited waveform synthesis was first introduced by Stilson and Smith in 1996 [14]. They noted that by differentiating (twice in the case of the triangle wave) a continuous-time classical waveform with respect to time one obtains a sequence of impulse functions (with a DC offset in the case of the sawtooth wave). For example, differentiation of a rectangular pulse wave that has a duty cycle $P$ yields

$$\frac{\mathrm{d}}{\mathrm{d}t} r(t; P) = 2 \sum_{k=-\infty}^{\infty} \left( \delta(t - kT_0) - \delta(t - (k + P)T_0) \right), \quad (1)$$

where $t$ is the time variable (in seconds), $T_0 = 1/f_0$ is the oscillation period in seconds and $\delta(x)$ is the Dirac delta (impulse) function that is zero when $x \neq 0$ and that satisfies the condition

$$\int_{-\infty}^{\infty} \delta(x)\,\mathrm{d}x = \int_{0-}^{0+} \delta(x)\,\mathrm{d}x = 1. \quad (2)$$

Now, by filtering the impulse train with a lowpass filter, every impulse of the sequence is replaced with the impulse response of the lowpass filter [14, 15]. This bandlimited impulse train (BLIT) can be synthesized in the digital domain by computing the impulse response values. After the impulse response values have been generated, the resulting impulse train is (numerically) integrated (again, twice in the case of the triangle wave) to obtain the bandlimited waveform [14, 15].

When the lowpass filter is ideal, the BLIT approach effectively produces the same result as the ideally bandlimited oscillator algorithms [14, 15]. However, since the impulse response of the ideal lowpass filter is the well-known $\mathrm{sinc}$ function,

$$h_{\mathrm{id}}(t) = 2f_{\mathrm{c}}\mathrm{sinc}(2f_{\mathrm{c}}t) = \frac{\sin(2\pi f_{\mathrm{c}}t)}{\pi t}, \quad (3)$$

where $f_{\mathrm{c}}$ is the cutoff frequency of the filter, the ideal BLIT approach is unimplementable. Because the $\mathrm{sinc}$ function is infinitely long, infinitely many values would be required to be summed at every sampling instant [14, 15]. Therefore, approximations of the ideal bandlimited impulse function have been proposed.

Stilson and Smith proposed that the $\mathrm{sinc}$ function, the basis function of the BLIT approach, is windowed to get an implementable algorithm [14]. The windowed $\mathrm{sinc}$ function is then sampled and tabulated, and the impulse response values are read from the table in the BLIT synthesizer [7, 14, 15]. However, to obtain a good alias reduction performance the table needs to be quite long [7, 16, 17]. Furthermore, since the oscillation period $T_0$ can be arbitrary, the impulses can be located arbitrarily between the sampling points. This means that the tabulated impulse function needs to be oversampled to achieve improved accuracy in computing the impulse function values from the table entries [7, 14, 15].

Recently, it has been shown that the alias reduction performance of the table-based BLIT algorithm can be improved by sampling a controllable function or by optimizing the table entries by minimizing a perceptually informed cost function when the table is short [17]. Because of the poor performance of the windowed $\mathrm{sinc}$ function, various alternative basis functions have been proposed. These other approximations improve the alias reduction performance significantly compared to the performance of the windowed $\mathrm{sinc}$ function of the same effective length. These improved basis function generators utilize modified frequency modulation [18], feedback delay loops [19, 20], and fractional delay filters [8, 13, 20] as the method to approximate the ideal bandlimited impulse function.

Unfortunately, the BLIT approach can suffer from numerical problems that are caused by the integration process required to produce the actual waveform. If the impulse response values are not exact, the integration may cause the output to have a drifting DC component. To overcome this issue, Brandt suggested that the integration is performed with a second-order leaky integrator that blocks the DC component and that approximates the integrator well at other frequencies [21].

Furthermore, Brandt suggested that the DC issue of the BLIT approach can be avoided by integrating the BLIT basis function in advance [21]. This proposal is justified by the fact that the integration of a continuous-time non-bandlimited impulse train results in a sequence of step functions. Using this approach, the rectangular pulse waveform is expressed as

$$r(t; P) = 2 \sum_{k=-\infty}^{\infty} \left( u(t - kT_0) - u(t - (k + P)T_0) \right) - 1, \quad (4)$$

where $u(x)$ is the Heaviside unit step function

$$u(x) = \int_{-\infty}^{x} \delta(\tau)\,\mathrm{d}\tau = \begin{cases} 0, & \text{for } x < 0, \\ 0.5, & \text{for } x = 0, \text{and} \\ 1, & \text{for } x > 0. \end{cases} \quad (5)$$

By applying the same reasoning as for the bandlimited impulse function train, integration of the ideal BLIT basis function results in an ideal bandlimited unit step function that can be used to synthesize the bandlimited waveform directly [21].

The ideal bandlimited step function, i.e. the integral of the sinc function and hence the basis function of the bandlimited step function (BLEP) approach, can also be expressed in closed form as [12]

$$h_{\mathrm{Iid}}(t) = \int_{-\infty}^{t} 2f_{\mathrm{c}}\mathrm{sinc}(2f_{\mathrm{c}}\tau)\,\mathrm{d}\tau = \frac{1}{2} + \frac{1}{\pi}\mathrm{Si}(2\pi f_{\mathrm{c}}t), \quad (6)$$

where $\mathrm{Si}(x)$ is a function called the Sine integral [22]. Like the sinc function, the ideal BLEP basis function is also infinitely long. Therefore, it also needs to be approximated to have an implementable BLEP synthesizer. Again, approximations of the ideal BLEP basis function have been developed.

Brandt suggested that the minimum-phase representation of the windowed sinc function is accumulated to produce an approximation of the bandlimited step function [21]. Other basis functions proposed for the task utilize tabulated correction functions [23] and polynomial functions [7, 12, 13, 16, 24], some of which are in fact integrals of the basis functions proposed for the fractional delay filter BLIT oscillator.

Now, note that the basis functions of the BLIT and BLEP methods are linear-phase. Although the basis functions approximations do not necessarily need to be linear-phase, most of the existing ones are. The only nonlinear-phase approximations are generated by the allpass fractional delay filter BLIT oscillator [8], the feedback delay loop BLIT oscillator [19], and by the accumulated minimum-phase windowed-sinc function approximation [21].

The allpass fractional delay filter BLIT oscillator [8] and the feedback delay loop BLIT oscillator [19] both use allpass fractional delay filters as a part of the impulse generation algorithm. However, allpass filters do not have a well-defined continuous-time representation of their outputs. Therefore, these approaches can only be loosely interpreted to generate a nonlinear-phase approximation of the BLIT basis function.

The minimum-phase algorithm proposed by Brandt [21], on the other hand, is much closer to the idea of having a nonlinear-phase basis function than the other approaches. The minimum-phase representation of the BLIT basis function was, however, computed from the windowed and sampled sinc function approximation [21]. Therefore, it cannot be considered to be a direct nonlinear-phase basis function as is.

## 3. TIME-INVARIANT NONLINEAR-PHASE BASIS FUNCTIONS

Clearly, the desired basis functions have a lowpass-type amplitude response. While there are direct discrete-time methods with which digital lowpass filters that have nonlinear-phase response can be designed [25], the digital filters are typically designed using transformed analog filter design techniques. In such methods, the amplitude response of the filter is designed in the continuous-time domain using well-established analog filter design techniques. Then, the digital representation of this basis function, which is efficiently generated with a recursive digital filter, is obtained by transforming the analog filter into digital domain using an appropriate transformation method [25].

It should be noted that the unit step response of a filter is the integral of the filter's impulse response. This relation means that the BLEP basis functions can be interpreted to be integrated BLIT basis functions. Therefore, the discussion given henceforth is applied only to BLIT basis functions because the derivation for the BLEP basis function does not differ greatly from the derivation for the BLIT basis functions.

The common transformation methods include the impulse invariance, the bilinear transform, and the matched $z$-transform techniques. The impulse invariance method maps the continuous-time impulse response of an analog filter into a digital filter that generates sampled values of the analog response [26]. Effectively, the frequency response of the analog filter is aliased due to the sampling process.

The bilinear transform, on the other hand, maps the frequency response of the analog filter to the baseband of the digital system [25]. The matched $z$-transform maps the poles and zeros of the analog filter to poles and zeros of a digital filter that has approximately the same frequency response as the analog filter in the baseband [15, 27].

After a digital filter whose output is the desired basis function is obtained, the bandlimited sequence of basis functions can be generated by triggering the filter every time a discontinuity is detected. The discontinuities are detected by looking for large changes in the waveform (in case of sawtooth and rectangular pulse wave) or in the waveform derivative (in case of triangle wave). However, since the discontinuities are in general not at specific sampling instants, they can be detected at the instant following the discontinuity. Hence, the triggering can only happen at the sampling instants following the discontinuities, which means that the generated basis function is slightly delayed with respect to the actual discontinuity location.

Obviously, the discontinuity detection can be developed to be predictive, i.e. the algorithm could detect the discontinuity before it will happen. However, also this approach would cause the generated basis functions to be misaligned in time. Therefore, predictive discontinuity detection does not provide any improvements to the trivial (post-discontinuity detection) approach.

In general, the delay of the generated basis functions varies from a discontinuity to another. Due to the discontinuity-dependent delay, the approach described above causes the oscillation period to vary erratically around its nominal value. The period dithering does not reduce aliasing much and it introduces frequencies that should not be present in the waveform.

An example of the dithering effects is given in Fig. 2 where the spectra of the basis function train and the rectangular pulse wave generated with the described time-invariant technique are plotted. In this example, $f_0 = 3$ kHz, $f_{\mathrm{s}} = 44.1$ kHz, and the filter that generates the basis functions is a fourth-order Butterworth filter whose cutoff frequency is 75% of the Nyquist limit and that has been transformed to a digital filter with the impulse invariance technique. The rectangular pulse waveform (having a duty cycle of 25%) was generated by summing time-shifted step responses of the filter.

Figure 2 shows that the produced signals still contain a lot of aliasing. By comparing Figs. 2(b) and 1(b) one can see that the aliasing distortion of the rectangular pulse wave is not reduced much. Moreover, the fourth harmonic that should not be present due to the particular choice of duty cycle has a substantial amplitude and the relative levels of the non-aliased harmonics are not as they should be (see Fig. 1(b)).

It should be noted that the issues of the period dithering happen with every transformation technique. To overcome these issues, an extended technique that allows arbitrarily sampled discrete-time basis functions is developed next.

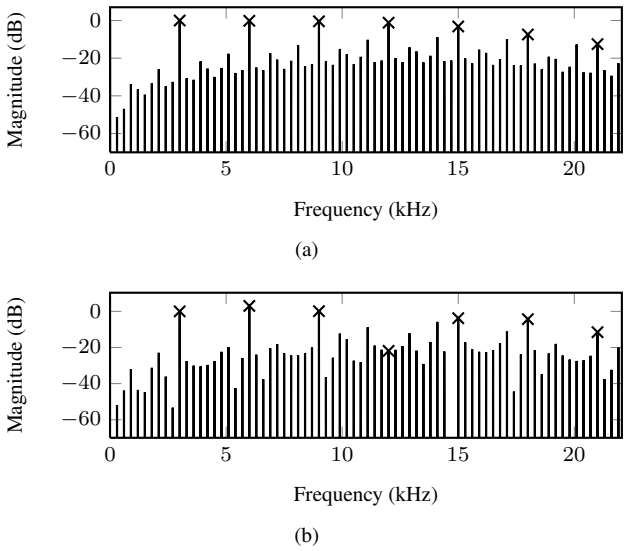


Figure 2: (a) Spectrum of the basis function train and (b) the spectrum of the rectangular pulse wave generated with the time-invariant technique. The crosses indicate the non-aliased components. The fundamental frequency $f_0 = 3$ kHz, the sampling frequency $f_\mathrm{s} = 44.1$ kHz, and the filter that generates the basis functions is a fourth-order Butterworth filter whose cutoff frequency is 75% of the Nyquist limit and that has been transformed to a digital filter with the impulse invariance technique. The rectangular pulse waveform (having a duty cycle of 25%) was generated by summing time-shifted, impulse-invariance transformed step responses of the analog prototype filter.

## 4. TIME-VARYING NONLINEAR-PHASE BASIS FUNCTIONS

### 4.1. Description of the Proposed Technique

Of the filter transformation techniques mentioned above, only the impulse invariance method enables the discrete-time impulse response to be generated at arbitrary time shifts. The bilinear and matched $z$-transform apply the transformation in the pole-zero domain and therefore they do not have a well-defined continuous-time impulse response that they can be understood to sample.

The time-varying extension of the impulse invariance method starts, like the time-invariant technique, by deriving the partial fraction expansion of the transfer function of the analog filter [26]. Because the underlying analog filter is a lowpass filter, the order of the transfer function denominator is lower that the order of its numerator. Therefore, the analog transfer function $H(s)$ can be decomposed into first-order sections,

$$H(s) = \sum_{k=1}^{N} \frac{r_k}{s - s_k}, \tag{7}$$

where $N$ is the filter order, $s_k$ are the filter poles, and $r_k$ are constants that depend on the filter zeros. If the filter poles are simple, the corresponding impulse response is given by

$$h_\mathrm{c}(t) = \begin{cases} \sum_{k=1}^{N} r_k e^{s_k t}, & \text{for } t \geq 0 \\ 0, & \text{otherwise.} \end{cases} \tag{8}$$

The decomposition of the Laplace transform $\hat{H}(s)$ of the BLEP basis function is easily derived from that of the BLIT basis function as

$$\hat{H}(s) = \frac{1}{s} H(s) = \frac{H(0)}{s} + \sum_{k=1}^{N} \frac{r_k / s_k}{s - s_k} \tag{9}$$

with the same $s_k$ and $r_k$ as above. Note that typically $H(0) = 1$. Then, it follows for the step response

$$\hat{h}_\mathrm{c}(t) = \begin{cases} 1 + \sum_{k=1}^{N} \frac{r_k}{s_k} e^{s_k t}, & \text{for } t \geq 0 \\ 0, & \text{otherwise.} \end{cases} \tag{10}$$

When (8) is sampled at time instants $t = nT$, where $T$ is the sampling interval in seconds and $n \in \mathbb{Z}$, the time-invariant impulse invariance transformation is obtained. In the time-varying case, the sampling occurs at instants $t = (n + d)T$, where $d \in [0, 1)$ is the offset (the fractional delay) from the beginning of the response (the time instant of the discontinuity) to the sampling instant following it (see [12] for more information about the offset computation). This time-shifted sampling results in a discrete-time impulse response expressed as

$$\begin{aligned} h(n, d) \equiv h_\mathrm{c}((n + d)T) &= \begin{cases} \sum_{k=1}^{N} r_k e^{s_k (n+d) T}, & \text{for } n \in \mathbb{N}_0, \\ 0, & \text{otherwise,} \end{cases} \\ &= \begin{cases} \sum_{k=1}^{N} r_k e^{s_k d T} e^{s_k n T}, & \text{for } n \in \mathbb{N}_0, \\ 0, & \text{otherwise,} \end{cases} \\ &= \begin{cases} \sum_{k=1}^{N} r_k z_k^d z_k^n, & \text{for } n \in \mathbb{N}_0, \\ 0, & \text{otherwise,} \end{cases} \end{aligned} \tag{11}$$

where the last expression was obtained with a substitution $z_k = e^{s_k T}$. Applying the $z$-transform to (11) gives the discrete-time filter

$$H(z, d) = \sum_{k=1}^{N} \frac{r_k z_k^d}{1 - z_k z^{-1}} \tag{12}$$

for the BLIT case, and, by similar means,

$$\hat{H}(z, d) = \frac{1}{1 - z^{-1}} + \sum_{k=1}^{N} \frac{\frac{r_k}{s_k} z_k^d}{1 - z_k z^{-1}} \tag{13}$$

for the BLEP case. Note that the additional $1/(1 - z^{-1})$ term represents a discrete step function.

Since the application area discussed here comprises real-valued systems and signals, (12) can be reformulated by combining the

sections that correspond to complex conjugate $r_k$ and $z_k$, yielding

$$H_{\mathfrak{Re}}(z,d) = \sum_{k=1}^{N_2} \frac{2\mathfrak{Re}\{r_{k,2} z_{k,2}^{d}\} - 2\mathfrak{Re}\{r_{k,2} z_{k,2}^{d-1}\}|z_{k,2}|^2 z^{-1}}{1 - 2\mathfrak{Re}\{z_{k,2}\}z^{-1} + |z_{k,2}|^2 z^{-2}} + \sum_{k=1}^{N_1} \frac{r_{k,1} z_{k,1}^{d}}{1 - z_{k,1} z^{-1}}, \quad (14)$$

where $r_{k,1}$ and $z_{k,1}$ are the $N_1$ real-valued numerator coefficients and poles, respectively, and $r_{k,2}$ and $z_{k,2}$ are a coefficient and pole pair of each $N_2$ complex conjugate pairs.

It can be noted that the recursive parts of (14) do not depend on $d$. Therefore, the time-shifted impulse response can be triggered at time instant $t_\mathrm{p} = (n_\mathrm{p} - d_\mathrm{p})T$ by exciting constituting filters

$$\bar{H}_{k,1}(z) = \frac{1}{1 - z_{k,1} z^{-1}}, \text{ and} \quad (15)$$

$$\bar{H}_{k,2}(z) = \frac{1}{1 - 2\mathfrak{Re}\{z_{k,2}\}z^{-1} + |z_{k,2}|^2 z^{-2}}, \quad (16)$$

with the respective input signals

$$u_{k,1}(n, d_\mathrm{p}) = \begin{cases} r_{k,1} z_{k,1}^{d_\mathrm{p}}, & \text{for } n = n_\mathrm{p}, \\ 0, & \text{otherwise}, \end{cases} \quad (17)$$

$$u_{k,2}(n, d_\mathrm{p}) = \begin{cases} 2\mathfrak{Re}\{r_{k,2} z_{k,2}^{d_\mathrm{p}}\}, & \text{for } n = n_\mathrm{p}, \\ -2\mathfrak{Re}\{r_{k,2} z_{k,2}^{d_\mathrm{p}-1}\}|z_{k,2}|^2, & \text{for } n = n_\mathrm{p} + 1, \\ 0, & \text{otherwise}, \end{cases} \quad (18)$$

and by summing their outputs. A sequence of impulse responses can be generated by superimposing input signals $u_{k,1}(n, d_\mathrm{p})$ and $u_{k,2}(n, d_\mathrm{p})$ for different pulse trigger times $t_\mathrm{p}$, yielding the set of driving signals $u_{k,1}(n)$ and $u_{k,2}(n)$. The block diagram of this approach is depicted in Fig. 3. To obtain a BLEP generator instead, we only need to divide the driving signals by the respective constants $s_{k,\{1,2\}}$ and add a simple discrete step function to the output with onset at $n_\mathrm{p}$, indepent of $d_\mathrm{p}$.

Note that the driving signals $u_{k,1}(n)$ and $u_{k,2}(n)$ will be sparse as the individual input signals contain only one or two nonzero values per pulse. Nevertheless, direct evaluation of (17) and (18) is unattractive as it requires computation of $N_1$ real and $N_2$ complex exponentials. However, they can be efficiently approximated with low-order polynomials, as shown in the following examples.

### 4.2. Design examples

To illustrate the approach described above, consider an analog lowpass prototype that has been designed as a fifth-order elliptic (Cauer) filter with a passband ripple of 1 dB, cutoff frequency at 75% of the Nyquist limit (corresponding to about 16.5 kHz for $f_\mathrm{s} =$ 44.1 kHz) and a stopband attenuation of 81 dB. The coefficients of the filter

$$H(s) = \frac{\sum_{m=0}^{5} b_m s^m}{\sum_{m=0}^{5} a_m s^m} \quad (19)$$

are given in Table 1.

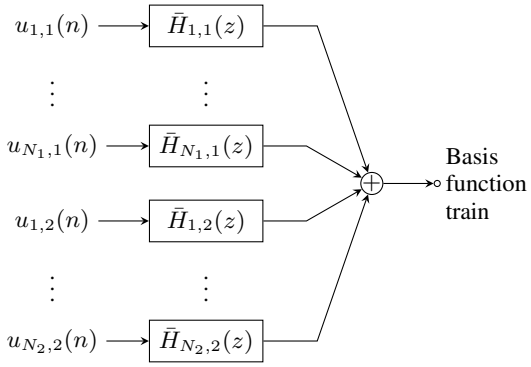


Figure 3: Block diagram of the basis function train generator.

Table 1: Coefficients of the fifth-order elliptic prototype analog lowpass filter.

| $m$ | $a_m$ | $b_m$ |
|---|---|---|
| 5 | 1.0000 | 0.00000 |
| 4 | 2.2012 | 0.00256 |
| 3 | 9.5082 | 0.00000 |
| 2 | 13.0517 | 0.35220 |
| 1 | 18.8744 | 0.00000 |
| 0 | 9.8924 | 9.89239 |

With the transformation method described above, the coefficients of the discrete-time system are given as

$$\begin{cases} z_{1,1} = 0.48986, \\ r_{1,1} = 0.78264, \end{cases} \quad (20)$$

$$\begin{cases} z_{1,2} = -0.57101 + 0.59345j, \\ r_{1,2} = 0.15963 + 0.12702j, \end{cases} \quad (21)$$

$$\begin{cases} z_{2,2} = 0.04685 + 0.57524j, \\ r_{2,2} = -0.54967 - 0.20284j, \end{cases} \quad (22)$$

that is, the system is composed of one first-order subsystem,

$$\bar{H}_{1,1}(z) = \frac{1}{1 - 0.48986 z^{-1}}, \quad (23)$$

and of two second-order subsystems,

$$\bar{H}_{1,2}(z) = \frac{1}{1 + 1.14202 z^{-1} + 0.67824 z^{-2}}, \text{ and} \quad (24)$$

$$\bar{H}_{2,2}(z) = \frac{1}{1 - 0.09369 z^{-1} + 0.33309 z^{-2}}. \quad (25)$$

When these systems are driven by the exact excitation signals as given by (17) and (18), the results depicted in Fig. 4 are obtained. As can be seen in Fig. 4(a), the amplitudes of the aliased components (as well as the wanted harmonics) of the impulse train directly depend on the amplitude response of the prototype lowpass, and that the "floor" level of the aliasing distortion approximately matches the stopband attenuation of the prototype lowpass filter.

To obtain the rectangular pulse wave, two appropriately time-shifted excitation signals with opposite sign were superimposed

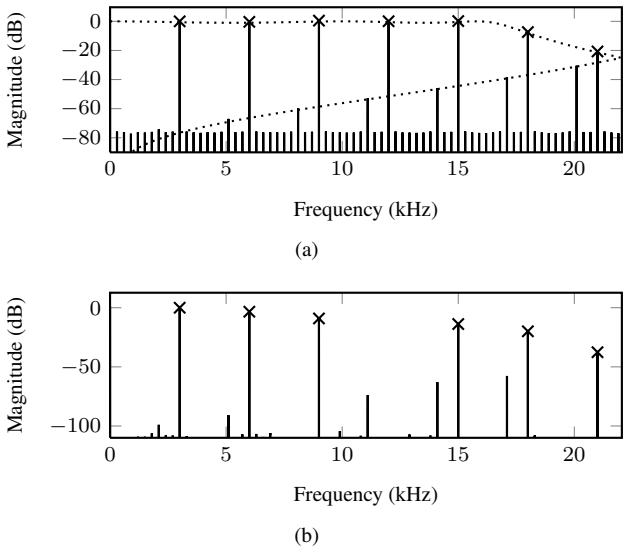


Figure 4: (a) Spectrum of the basis function train and (b) the spectrum of the rectangular pulse wave generated with the time-varying technique. The analog prototype filter is a fifth-order elliptic filter that has a cutoff frequency at 75% of the Nyquist limit, passband ripple of 1 dB, and stopband attenuation of 81 dB. As before, $f_0 =$ 3 kHz and $f_\mathrm{s} = 44.1$ kHz. Exact excitation signals are used. The dotted line in (a) represents the aliased magnitude response of the prototype filter. The rectangular pulse was synthesized using the BLEP generator algorithm.

and fed into the BLEP generator. As shown in Fig. 4(b), the additional roll-off of the integrated analog lowpass filter further helps in suppressing aliasing.

By examining the dependency between the offset $d$ and the excitation signals (17) and (18), it is observed that these functions are typically relatively smooth. For instance, the exact excitation signals for the filter coefficients of (20)–(22), plotted in Fig. 5, can be approximated well with third-order polynomials

$$u_{k,1}(n, d_\mathrm{p}) \approx \begin{cases} \sum_{l=0}^{3} c_{k,1,l} d_\mathrm{p}^l, & \text{for } n = n_\mathrm{p}, \\ 0, & \text{otherwise}, \end{cases} \tag{26}$$

$$u_{k,2}(n, d_\mathrm{p}) \approx \begin{cases} \sum_{l=0}^{3} c_{k,2,0,l} d_\mathrm{p}^l, & \text{for } n = n_\mathrm{p}, \\ \sum_{l=0}^{3} c_{k,2,1,l} d_\mathrm{p}^l, & \text{for } n = n_\mathrm{p} + 1, \\ 0, & \text{otherwise}, \end{cases} \tag{27}$$

for $k = 1, 2$. Performing a least-squares fit of the exact signals, the coefficients listed in Table 2 are obtained. These polynomials yield good results, as can be seen in the resulting spectra plotted in Fig. 6. The desired harmonics and the most prominent aliased components are nearly unaffected by this approximation. The major difference lies in an increase of the higher-order aliasing distortion at high frequencies.

Obviously, by choosing the filter order and the order of the polynomial approximation appropriately, one obtains different trade-offs between accuracy and computational complexity. This is illustrated

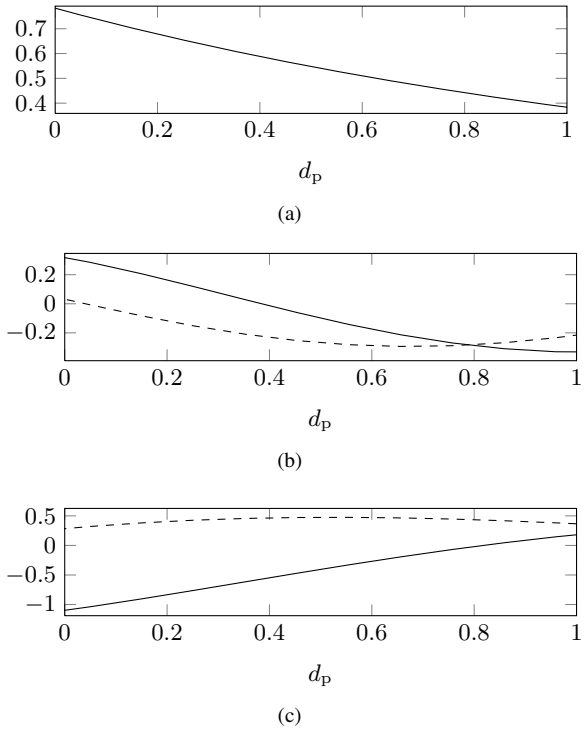


Figure 5: Exact excitation signal values as a function of the offset $d_\mathrm{p}$: (a) $u_{1,1}(n_\mathrm{p}, d_\mathrm{p})$, (b) $u_{1,2}(n_\mathrm{p}, d_\mathrm{p})$ (solid line) and $u_{1,2}(n_\mathrm{p} + 1, d_\mathrm{p})$ (dashed line), and (c) $u_{2,2}(n_\mathrm{p}, d_\mathrm{p})$ (solid line) and $u_{2,2}(n_\mathrm{p} + 1, d_\mathrm{p})$ (dashed line).

Table 2: Coefficients for the third-order polynomial approximation of the exact excitation signal values.

| $l$ | $c_{1,1,l}$ | $c_{1,2,0,l}$ | $c_{1,2,1,l}$ | $c_{2,2,0,l}$ | $c_{2,2,1,l}$ |
|---|---|---|---|---|---|
| 3 | −0.0334 | 0.6444 | 0.1564 | −0.4882 | 0.2008 |
| 2 | 0.1909 | −0.5921 | 0.4788 | 0.5123 | −0.9012 |
| 1 | −0.5567 | −0.7035 | −0.8831 | 1.2570 | 0.7820 |
| 0 | 0.7826 | 0.3219 | 0.0362 | −1.1017 | 0.2837 |

by Figs. 7 and 8. In Fig. 7, a seventh-order elliptic filter, which has the same design parameters as the previous example, was combined with fifth-order polynomial approximation to obtain results with very low distortion. In contrast, Fig. 8 shows the spectra of a case where a third-order Butterworth filter, which has its cutoff frequency at 75 % of the Nyquist frequency, was combined with first-order polynomial (i.e. linear) approximation of the excitation signals. As expected, the aliasing distortion is increased but the result might still be good enough in applications where computational efficiency is a main priority.

## 5. CONCLUSIONS AND FURTHER WORK

In virtual analog synthesis, special attention needs to be given to the generation of bandlimited source signals. An efficient methodology for the synthesis of bandlimited waveforms typically used in virtual analog synthesis is based on expressing the waveform or its time-

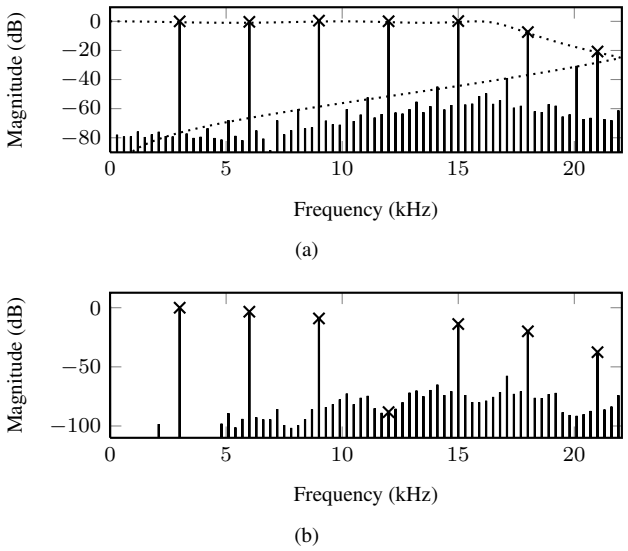


Figure 6: (a) Spectrum of the basis function train and (b) the spectrum of the rectangular pulse wave generated with the time-varying technique using the fifth-order elliptic prototype filter and third-order polynomial approximations of the exact excitation signals.

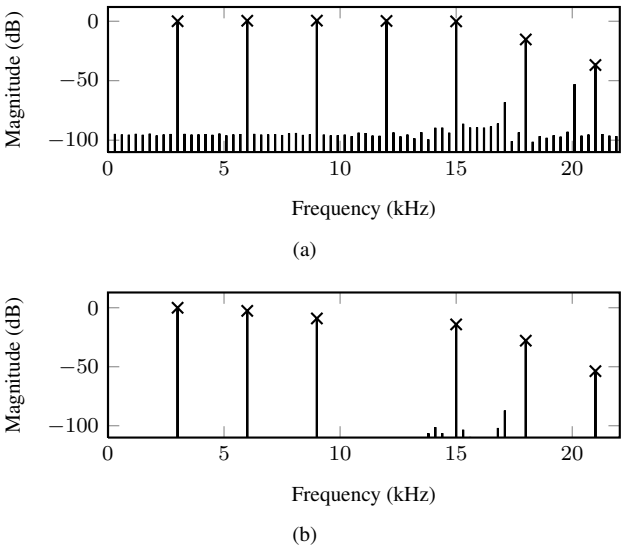


Figure 7: (a) Spectrum of the basis function train and (b) the spectrum of the rectangular pulse wave generated with the time-varying technique when the prototype filter is a seventh-order elliptic filter and the excitation signals are approximated with fifth-order polynomials. Again, $f_0 = 3$ kHz, $f_s = 44.1$ kHz, the crosses indicate the non-aliased components, and the rectangular pulse wave is synthesized with the BLEP generator.

derivative as a sequence of bandlimited impulse or step functions. By doing so, the algorithms of this group effectively reduce the aliasing distortion present in the waveforms. Because the ideal bandlimited functions, i.e. the ideal basis functions of these quasi-bandlimited oscillator algorithms, are infinitely long, alternative basis functions that are implementable have been suggested.

So far, the basis functions proposed for the task have been linear-phase functions apart from a couple of special cases. In this paper, a general technique for deriving nonlinear-phase basis function generators was discussed. The proposed algorithm is based on transforming the impulse or step response of an analog filter to a digital filter using a modified impulse invariance transformation method. The modified transformation enables arbitrary (sub-sample) offsets to be done to the filter's response, thus fulfilling the need of shiftable basis functions in the quasi-bandlimited oscillator algorithms.

The resulting digital filter obtained with the proposed technique is essentially a set of parallel first- and/or second-order IIR filters that are excited with short burst-like signals. The excitation signals that have one or two nonzero values depend on the needed sub-sample offset. The exact expressions of the excitation signals have complex exponentials, but it was shown that they can efficiently be approximated with low-order polynomials. The choice of filter and polynomial order thus allows a flexible trade-off between aliasing reduction and computational complexity.

The nonlinearity of the phase response was assumed to yield inaudible effects in the description of the discussed technique. However, while this may be the case in general, further analysis of the effects of the nonlinearity of the phase response should be still performed. Furthermore, the proposed method was exemplified with various design cases. In order to have practical choices for the analog prototype filter, design rules should be derived using the latest knowledge of the audibility of aliasing. Moreover, the proposed technique should be compared with the existing approximations in

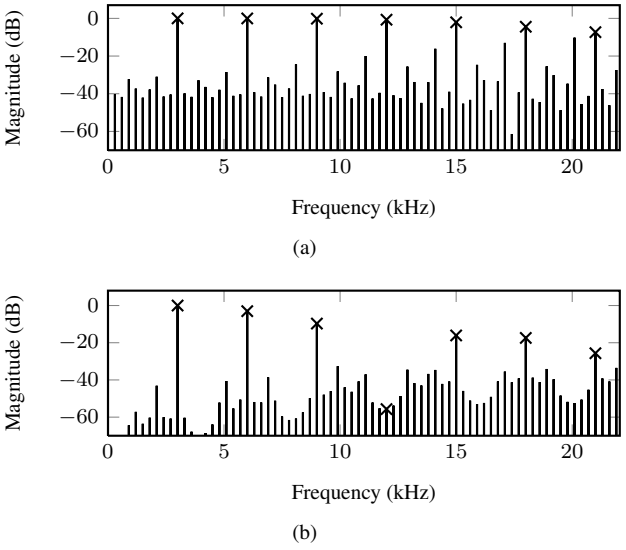


Figure 8: (a) Spectrum of the basis function train and (b) the spectrum of the rectangular pulse wave generated with the time-varying technique when the prototype filter is a third-order Butterworth filter and the excitation signals are approximated with first-order (linear) polynomials. Again, $f_0 = 3$ kHz, $f_s = 44.1$ kHz, the crosses indicate the non-aliased components, and the rectangular pulse wave is synthesized with the BLEP generator.

terms of aliasing reduction and computational complexity.

Sound and code examples of the presented approach can be found online at the paper's companion page `http://pekonen.cc/p/dafx12-nlpo/`.

## 6. ACKNOWLEDGMENTS

This work was started when J. Pekonen was with the Department of Signal Processing and Acoustics, Aalto University School of Electrical Engineering. His work was in part supported by the Academy of Finland, project no. 122815.

The authors would like to thank Julian Parker for his insightful comments.

## 7. REFERENCES

[1] H. F. Olson, H. Belar, and J. Timmens, "Electronic music synthesis," *J. Acoust. Soc. Am.*, vol. 27, no. 3, pp. 595–612, May 1955.

[2] R. A. Moog, "Voltage-controlled electronic music modules," *J. Audio Eng. Soc.*, vol. 13, no. 3, pp. 200–206, July 1965.

[3] H. G. Alles, "Music synthesis using real time digital techniques," *Proc. IEEE*, vol. 68, no. 4, pp. 436–449, Apr. 1980.

[4] H. Chamberlin, *Musical Applications of Microprocessors*, chapter 13, pp. 418–480, Hayden Book Company, Hasbrouck Heights, NJ, 2nd edition, 1985.

[5] F. R. Moore, *Elements of Computer Music*, Prentice Hall, Englewood Cliffs, NJ, 1990.

[6] M. Puckette, *The Theory and Technique of Electronic Music*, pp. 301–322, World Scientific Publishing Co., Hackensack, NJ, 2007.

[7] V. Välimäki and A. Huovilainen, "Antialiasing oscillators in subtractive synthesis," *IEEE Signal Process. Mag.*, vol. 24, no. 2, pp. 116–125, Mar. 2007.

[8] J. Nam, V. Välimäki, J. S. Abel, and J. O. Smith, "Efficient antialiasing oscillator algorithms using low-order fractional delay filters," *IEEE Trans. Audio, Speech, and Lang. Process.*, vol. 18, no. 4, pp. 773–785, May 2010.

[9] V. Välimäki, J. Nam, J. O. Smith, and J. S. Abel, "Alias-suppressed oscillators based on differentiated polynomial waveforms," *IEEE Trans. Audio, Speech, and Lang. Process.*, vol. 18, no. 4, pp. 786–798, May 2010.

[10] V. Lazzarini and J. Timoney, "New perspectives on distortion synthesis for virtual analog oscillators," *Computer Music J.*, vol. 34, no. 1, pp. 28–40, Spring 2010.

[11] J. Pekonen and V. Välimäki, "The brief history of virtual analog synthesis," in *Proc. 6th Forum Acusticum*, Aalborg, Denmark, June 2011, pp. 461–466.

[12] V. Välimäki, J. Pekonen, and J. Nam, "Perceptually informed synthesis of bandlimited classical waveforms using integrated polynomial interpolation," *J. Acoust. Soc. Am.*, vol. 131, no. 1, part 2, pp. 974–986, Jan. 2012.

[13] J. Pekonen, J. Nam, J. O. Smith, and V. Välimäki, "Optimized polynomial spline basis function design for quasi-bandlimited classical waveform synthesis," *IEEE Signal Process. Lett.*, vol. 19, no. 3, pp. 159–163, Mar. 2012.

[14] T. Stilson and J. O. Smith, "Alias-free digital synthesis of classic analog waveforms," in *Proc. Int. Computer Music Conf.*, Hong Kong, China, Aug. 1996, pp. 332–335.

[15] T. Stilson, *Efficiently-Variable Non-Oversampling Algorithms in Virtual-Analog Music Synthesis — A Root-Locus Perspective*, Ph.D. thesis, Stanford Univ., Stanford, CA, June 2006, Available online `http://ccrma.stanford.edu/~stilti/papers/` (date last viewed July 10, 2012).

[16] J. Pekonen, "Computationally efficient music synthesis — Methods and sound design," M.Sc (Tech.) thesis, TKK Helsinki Univ. Tech., Espoo, Finland, June 2007, Available online `http://www.acoustics.hut.fi/publications/files/theses/pekonen_mst/` (date last viewed July 10, 2012).

[17] J. Pekonen, J. Nam, J. O. Smith, J. S. Abel, and V. Välimäki, "On minimizing the look-up table size in quasi bandlimited classical waveform synthesis," in *Proc. 13th Int. Conf. Digital Audio Effects (DAFx-10)*, Graz, Austria, Sept. 2010, pp. 57–64.

[18] J. Timoney, V. Lazzarini, and T. Lysaght, "A modified FM synthesis approach to bandlimited signal generation," in *Proc. 11th Int. Conf. Digital Audio Effects (DAFx-08)*, Espoo, Finland, Sept. 2008, pp. 27–33.

[19] J. Nam, V. Välimäki, J. S. Abel, and J. O. Smith, "Alias-free oscillators using feedback delay loops," in *Proc. 12th Int. Conf. Digital Audio Effects (DAFx-09)*, Como, Italy, Sept. 2009, pp. 347–352.

[20] J. Pekonen, V. Välimäki, J. Nam, J. S. Abel, and J. O. Smith, "Variable fractional delay filters in bandlimited oscillator algorithms for music synthesis," in *Proc. 2010 Int. Conf. Green Circuits and Systems (ICGCS2010)*, Shanghai, China, June 2010, pp. 148–153.

[21] E. Brandt, "Hard sync without aliasing," in *Proc. Int. Computer Music Conf.*, Havana, Cuba, Sept. 2001, pp. 365–368.

[22] M. Abramowitz and I. A. Stegun, Eds., *Handbook of Mathematical Functions with Formulas, Graphs, and Mathematical Tables*, pp. 231–232, U.S. Department of Commerce, Washington D.C., 1964.

[23] A. B. Leary and C. T. Bright, "Bandlimited digital synthesis of analog waveforms," U.S. Patent 7,589,272, Sept. 2009.

[24] Beat Frei, "Digital sound generation: Part I," Available online `http://www.icst.net/research/download/digital-sound-generation/` (date last viewed July 10, 2012), Feb. 2002.

[25] S. K. Mitra, *Digital Signal Processing: A Computer-Based Approach*, chapter 9.2, pp. 494–499, McGraw-Hill, New York, NY, 3rd international edition, 2005.

[26] L. B. Jackson, "A correction to impulse invariance," *IEEE Signal Process. Lett.*, vol. 7, no. 10, pp. 273–275, Oct. 2000.

[27] A. B. U. Athukorala and P. C. Perera, "Improved matched pole zero mapping method for design of discrete controllers," in *Proc. Int. Conf. Industrial and Information Systems (ICIIS 2007)*, Penadeniya, Sri Lanka, Aug. 2007, pp. 451–454.